



AIAA-2003-1748

Response Surface Approximation with Augmented
and Compactly Supported Radial Basis Functions

T. Krishnamurthy
NASA Langley Research Center,
Hampton, VA 23681

**44th AIAA/ASME/ASCE/AHS/ASC
Structures, Structural Dynamics, and
Materials Conference**

7-10 April, 2003
Norfolk, Virginia

For permission to copy or republish, contact the American Institute of Aeronautics and Astronautics
1801 Alexander Bell Drive, Suite 500, Reston, VA 22091

Response Surface Approximation with Augmented and Compactly Supported Radial Basis Functions

T. Krishnamurthy*

NASA Langley Research Center, Hampton, VA 23681, U. S. A.

Abstract:

A local response surface construction method based on augmented and compactly supported Radial Basis Functions (RBF) was developed. The developed method was tested in two numerical examples. The response surface generated using polynomial augmented RBF predict the response of a system better than the one constructed using classical RBF. The results obtained from the RBF based methods were also compared with the results obtained using local methods based on Moving Least Square (MLS) and kriging. It was found that all the three local methods (RBF, MLS, and kriging) predict the response with almost the same accuracy.

1. Introduction:

Structural reliability engineering analysis involves determination of probability of structural failure taking into account the uncertainty in the geometric parameters, material properties and loading conditions [1]. The uncertain quantities are treated as random variables and often a large number of simulations (structural analyses) with different sets of random variables are necessary to estimate the reliability of a structure. Hence the computational effort required to perform a structural reliability analysis can be very high. In order to minimize the computational time, response surface functions are often used as simple and inexpensive replacements for computationally expensive structural analyses in reliability methods. Most of the response surface construction methods use a single

quadratic or cubic polynomial to represent the entire parametric space of the random variables. These methods can be classified as global methods. Since the global methods use a single polynomial to represent the entire parametric space, they introduce large errors in the response estimation or limit the size of the parametric space. In order to overcome such difficulties, piecewise polynomial functions are often used. For example, finite element methods use piecewise polynomials. However, the piecewise polynomials for response surface construction are restricted to two- or three-dimensions. Hence, local methods were developed and presented as an alternate in response surface approximation [2], where it is possible to extend the method to arbitrary number of dimensions. In arriving at an interpolated value at some point in the parametric space, the local methods more heavily weight data samples that are "nearby" rather than giving all data samples equal weight.

A new local Moving Least Square (MLS) response surface construction method was developed in reference 2. The MLS method was compared with other local methods such as kriging [3] and found to be more accurate and computationally efficient. Another class of local response surface construction using Radial Basis Functions (RBF) is also widely used [4-6]. The complete description of these classical radial basis functions is available in reference 7. Recently, compactly supported radial functions were derived [8-10]. These functions are derived using the condition that the interpolation matrix should be positive definite.

* Aerospace Engineer, Analytical and Computational Methods Branch, Senior Member, AIAA

Copyright ©2001 by the American Institute of Aeronautics and Astronautics, Inc. No copyright is asserted in the United States under Title 17, U.S. Code. The U.S. Government has a royalty-free license to exercise all rights under the copyright claimed herein for Governmental Purposes. All other rights are reserved by the copyright owner

These compactly supported radial basis functions produce interpolation matrices that are sparse and for interpolation use only a few terms. Another advantage of compactly supported radial basis functions is that the data error in a single point or region does not affect the entire domain. It is known that classical radial basis functions and compactly supported radial basis functions do not reproduce exact values of constant and higher order polynomial terms in the interpolation [7]. To reproduce polynomial terms exact, the classical radial basis functions are augmented with polynomial terms. The effect of augmented polynomial terms to the newly developed compactly support radial basis functions on response surface generation is not investigated in the literature.

The objective of the present work is two fold: (a) to develop response surface approximation with augmented classical and compactly supported radial basis functions and (b) compare the radial based method with global, MLS and kriging based response construction methods. The effect of augmented polynomial terms on the accuracy of the response surface will be studied. The sampling points for the response surface construction will be selected using Progressive Lattice Sampling (PLS) experimental design [2].

First, the response surface construction method using radial basis functions is presented as part of the interpolation methods. Then a brief introduction to global, MLS and kriging methods of response surface construction is presented. Then the Progressive Lattice Sampling (PLS) method of selecting data points is provided. Next, the selected response surface construction methods are tested in a two variable problem and results are compared. Finally a four-variable example from a reliability application is presented to demonstrate the effectiveness of the augmented classical and compactly supported radial basis functions for response surface construction.

2. Interpolation Methods:

The accuracy of the response surface in representing the behavior of the actual system largely depends upon the interpolating method used for its generation. First, response surface generation using Radial Based Functions (RBF) is developed in this section. This is followed by a brief introduction (adopted from reference 2) to the Global Least Square (GLS), kriging and MLS interpolating methods.

2.1 Radial Basis Response Surface Construction

In this section, first the response surface construction method using classical RBF is described. Next, response surface construction using compactly supported RBF is presented. Finally, response surface construction using augmented RBF is described.

2.11 Classical RBF Response Surface Construction:

In classical RBF based methods, the interpolation of a surface $s(x)$ is performed as a linear combination of radial functions as

$$s(x) = \sum_{j=1}^N I_j \mathbf{j} \left(\|x - x_j\|_2 \right) \quad (1)$$

where the radial basis functions \mathbf{j} are functions of the radial distance $\|x - x_j\|_2$ from node j , I_j are interpolation constants to be determined, and N is the number of sample or data points with known function values F_j such that

$$s(x_j) = F_j \quad (2)$$

The Euclidean norm $\|x - x_j\|_2$ represents the radial distance r of the point x from the center x_j . For two-dimensional systems in Cartesian X-Y coordinates, the radial distance can be obtained as

$$\|x - x_j\|_2 = \sqrt{(X - X_j)^2 + (Y - Y_j)^2}$$

The unknown interpolation coefficients I_j in Equation (1) can be determined by minimizing the norm

$$J = \left[F_k - \sum_{j=1}^N I_j \mathbf{j} \left(\|x_k - x_j\|_2 \right) \right]^2 \quad \text{for } k = 1, 2, 3, \dots, N \quad (3)$$

The minimization equation in matrix form can be written as

$$[A]\{a\} = \{R\} \quad (4)$$

where

$$\{a\}^T = \{I_1, I_2, I_3, \dots, I_N\} \quad (5)$$

$$\{R\}^T = \{F_1, F_2, F_3, \dots, F_N\}$$

and the coefficient a_{ij} (i^{th} row and j^{th} column) of the matrix $[A]$ can be obtained from

$$a_{ij} = \mathbf{j} \left(\|x_i - x_j\|_2 \right) \quad (6)$$

Since, there are N equations with N unknown constants $I_j, j=1, N$; the resulting surface is an interpolating surface.

All the radial basis response surface construction methods use classical radial functions of the form of Equation (1). The response surface construction methods developed using classical RBF have the following limitations:

1. RBF does not possess compact support, i. e., change in any one of the center coordinates x_j affects the entire interpolation,
2. the system matrix $[A]$ in Equation (4) may not be positive definite [7], and
3. almost all the RBF can reproduce a constant function only in the limit as $N \rightarrow \infty$, i. e., number of sampling points is large.

Most commonly used radial classical radial functions are given in Table 1:

Table 1: Classical RBF Functions (from reference 4)

Classical RBF	Equation $r = \ x - x_j\ _2$
Linear	$f(r) = cr$
Cubic	$f(r) = (r + c)^3$
Thin plate spline	$f(r) = r^2 \log(cr^2)$
Gaussian	$f(r) = e^{-cr^2}$
Multiquadratic	$f(r) = (r^2 + c^2)^{\frac{1}{2}}$

The constant c in the radial basis functions in Table 1 is adjusted to obtain the best fit. However, there is no simple way to evaluate the constant c [6]. In the present work the constant c is set to unity except for the cubic function where it is set to zero.

2.12 Compactly Supported RBF Response Surface Construction:

Compactly supported radial functional are generated [8-10] recently. For compactly supported radial functions, the interpolation matrix $[A]$ in Equation (4) is sparse and positive definite. Also for interpolation only a few terms need to be considered. This leads to efficient algorithms for the computation and evaluation of response surfaces. In this study, the following two compactly supported radial functions are adapted from reference 7

Compact-I:

$$\begin{aligned} \mathbf{j}(r) &= (1-t)^5(8+40t+48t^2+25t^3+5t^4), & 0 \leq r \leq r_0 \\ &= 0 & r > r_0 \end{aligned} \quad (7)$$

Compact-II:

$$\begin{aligned} \mathbf{j}(r) &= (1-t)^6(6+36t+82t^2+72t^3+30t^4+5t^5), & 0 \leq r \leq r_0 \\ &= 0 & r > r_0 \end{aligned} \quad (8)$$

where $t = \frac{r}{r_0}$, and r_0 is the radius of the domain of

compact support. The compact support radius r_0 is a free parameter in the interpolation, and is selected by the user. Many other compact support functions are given in references 9 and 10.

The compactly supported radial basis function in Equations (7) or (8) is used in Equation (1) for response surface generation.

2.13 Augmented RBF Response Surface Construction

The classical RBF in Table 1 and the two compact support radial functions in Equations (7) and (8) can reproduce simple polynomials (constant, linear and quadratic etc.) only in the limit (i. e., as the number of sampling points increased). To illustrate this point, consider a one-dimensional problem with variable

$-1.0 \leq X_1 \leq 1.0$ and five equally spaced sampling points as shown in Figure 1. The function values at the five sampling points are set to a constant value of unity to verify the ability of various RBF to reproduce a constant function.

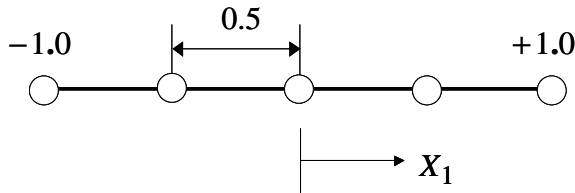


Figure 1. One-dimensional problem with five equally spaced sampling points

The responses predicted by the classical RBF and compactly supported RBF to the constant function are shown in Figures 2 and 3, respectively.

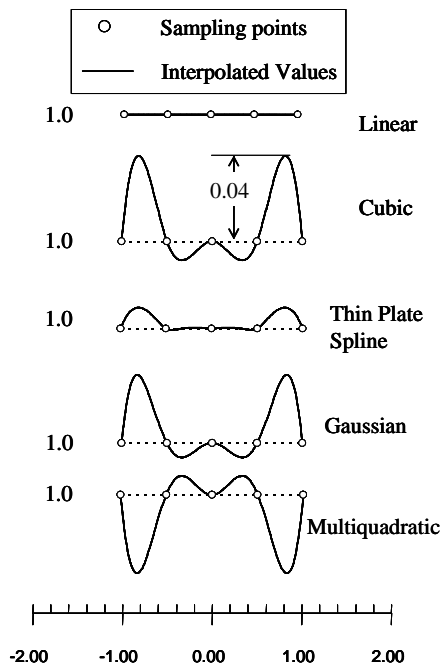


Figure 2. Response of classical Radial Basis Functions to a constant value

Clearly from Figures 2 and 3, except for the linear radial basis function, none of the other RBF, including the compactly supported RBF, can exactly reproduce the constant function. However, all the RBF can reproduce

the constant function for a sufficiently large number of sampling points.

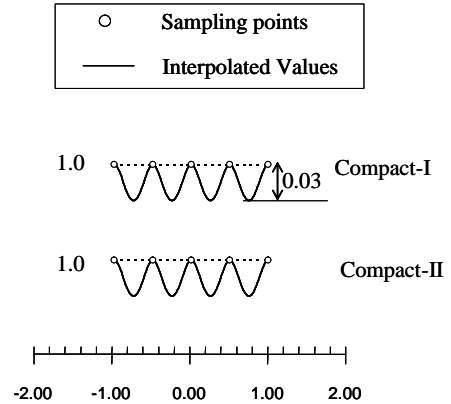


Figure 3. Response of compactly supported radial basis functions to a constant value

In order for the RBF to reproduce simple polynomials, the functions can be augmented by polynomial terms as

$$s(X) = \sum_{j=1}^N I_j f(r) + \sum_{i=1}^m P_i(x) b_i \quad (9)$$

where $P_i(x)$ are the monomial terms in the polynomials and b_i are the additional m constants introduced in the interpolation due to the polynomial terms. For two-dimensional problems, the monomial terms are $[1, x, y, x^2, xy, y^2, \dots]$.

The additional m unknown constants introduced in Equation (9) depend on the order of the polynomial selected and the order of the problem dimension d . The number of m unknown constants due to polynomial terms can be determined from

$$m = 1 \quad \text{for constant}$$

$$m = d + 1 \quad \text{for linear polynomial}$$

$$m = \frac{(d+1)(d+2)}{2} \quad \text{for quadratic polynomial}$$

$$m = \frac{(d+1)(d+2)(d+3)}{6} \quad \text{for cubic polynomial}$$

Equation (9) consists of N equations with $N + m$ unknowns. The additional m equations necessary to solve the m additional unknowns can be obtained from the following m constraints [7]

$$\sum_{j=1}^N P_i(x) \mathbf{I}_j \quad \text{for } i = 1, 2, 3, \dots, m \quad (11)$$

Hence, the polynomial augmented radial functions do not require any additional sampling points. The constraints in Equation (11) are handled internally in the interpolation. Equation (4) (to obtain the unknown constants) can be modified (using Equations (9) and (11)) for the augmented RBF as

$$\begin{bmatrix} [A]_{N \times N} & [B]_{N \times m} \\ [B]_{m \times N}^T & [0]_{m \times m} \end{bmatrix} \begin{Bmatrix} \{a\}_{N \times 1} \\ \{b\}_{m \times 1} \end{Bmatrix} = \begin{Bmatrix} \{R\}_{N \times 1} \\ \{0\}_{m \times 1} \end{Bmatrix} \quad (12)$$

where

$$\{b\}^T = \{b_1, b_2, b_3, \dots, b_m\} \quad (13)$$

and the coefficient b_{ij} (i^{th} row and j^{th} column) of the matrix $[B]$ can be obtained from

$$b_{ij} = P_j(x_i) \quad (14)$$

$j = 1, 2, \dots, m$ and $i = 1, 2, \dots, N$

Since, there are $N + m$ equations with $N + m$ unknown constants, the resulting surface constructed using augmented RBF is also an interpolating surface.

It is important to point out that, when augmented RBF is used to represent simple polynomials, the constant \mathbf{I}_j in Equation (9) will be identically zero. For non-polynomial functions, the polynomial terms are expected to augment the performance of the RBF.

2.2 Global Least Square Method (GLS)

The GLS methods are generally known as polynomial regression methods and are widely used in the literature (Refer 2 for additional references). The GLS methods are used to create response surface functions from a set

of sampling points. For example, a quadratic polynomial with d design variables has the form

$$s(x) = a_0 + \sum_{j=1}^d a_j x_j + \sum_{j=1, i=j}^d b_{ij} x_i x_j \quad (15)$$

Where $s(x)$ is the approximated value of the target function at the point in the parameter space having coordinates (x_1, x_2, \dots, x_d) , and a_0, a_j , and b_{ij} are the unknown constant coefficients. The unknown coefficients are determined by a regression procedure. Most commonly, the method of least squares is used to determine the coefficients that minimize the error of the approximation at the sampling points. Since a single polynomial is used to represent the entire parametric space, the method is termed here as the Global Least Squares (GLS) method. In the present study, the GLS method is limited to the quadratic polynomial given by Equation (15).

2.3 Kriging

Kriging is an interpolation method that originated in the geostatistics. Kriging uses the properties of the spatial correlation among the data samples. In arriving at an interpolated value at some point in the parameter space, kriging more heavily weights data samples that are “nearby” rather than giving all data samples equal weight. This is achieved by setting the mean residual error to zero and by minimizing the variance of the errors. The final equations for kriging are given below from reference 3 for N sampling points and d design variables:

The estimated value of s in kriging is obtained from

$$s(x) = \hat{\mathbf{b}} + r^T R^{-1} (\mathbf{y} - \hat{\mathbf{b}} \mathbf{f}) \quad (16)$$

where \mathbf{Y} is the column vector of known function values at the N sampling points, $\hat{\mathbf{b}}$ is a constant to be determined, R is correlation matrix obtained for an i^{th} row and j^{th} column from the correlation function as

$$R(x^i, x^j) = \exp \left[-\mathbf{q} \sum_{k=1}^d |x_k^i - x_k^j|^2 \right], \quad (17)$$

r is the column vector of length N obtained from

$$r^T = \{R(x, x^1), R(x, x^2), \dots, R(x, x^N)\}^T \quad (18)$$

and f is vector of length N , with all elements in the vector set to unity as

$$f^T = \{1, 1, 1, \dots, 1\}^T$$

The unknown $\hat{\mathbf{b}}$ in Equation (16) can be obtained from

$$\hat{\mathbf{b}} = (f^T R^{-1} f)^{-1} f^T R^{-1} Y \quad (19)$$

The Maximum Likelihood Estimate (MLE) for the unknown quantity \mathbf{q} in Equations (16) is obtained from a one-dimensional maximization problem defined by

$$\text{MLE} = \max \left(\frac{-1}{2} \right) [N \ln(\hat{\mathbf{S}}^2) + \ln|R|] \quad 0 \leq \mathbf{q} \leq \infty \quad (20)$$

Where

$$\hat{\mathbf{S}}^2 = \frac{(Y - \mathbf{b}f)^T R^{-1} (Y - \mathbf{b}f)}{N} \quad (21)$$

Estimation of \mathbf{q} in the one dimensional optimization problem is the critical step in the kriging method. The kriging method used in this study produces a C^2 continuous interpolating function over the entire parameter space. More details can be obtained from reference 3.

2.4. Moving Least Square (MLS) method

The Moving Least Squares (MLS) method is widely used in meshless methods [11,12]. Recently the MLS method has been successfully applied for response surface generation in the context of optimization in reference 13. A MLS method is briefly discussed here:

The MLS approximation for the estimated value $s(x)$ can be written as

$$s\{x\} = p^T\{x\} a_m(x) \quad (22)$$

where $p^T\{x\} = [p_1\{x\}, p_2\{x\}, \dots, p_m\{x\}]$ is a polynomial basis function of order m used in the MLS interpolation. The coefficients $a_j(x)$, $j=1,2,\dots,m$, are functions of

the spatial coordinates. For example, for two design variables,

$$p^T\{x\} = [1, x_1, x_2], \text{ Linear basis function; } m = 3$$

$$p^T\{x\} = [1, x_1, x_2, x_1^2, x_1 x_2, x_2^2], \text{ Quadratic basis function; } m = 6$$

The unknown coefficients a_m can be determined using the weighted least squares error norm $J(X)$ at the N sampling points

$$J(x) = \sum_{i=1}^N w_i(x) [P^T(x_i) a_m(x) - Y]^2 \quad (23)$$

$$= [P a_m(x) - Y]^T \cdot W \cdot [P a_m(x) - Y]$$

where $w_i(X)$ is weight function associated with node i , whose value is nonzero only in the support or influence domain of the node x_i (usually a sphere of radius R_i). The matrices P and W are defined as

$$P = \begin{Bmatrix} p^T(x_1) \\ p^T(x_2) \\ \dots \\ p^T(x_N) \end{Bmatrix}_{N \times m} \quad (24)$$

$$W = \begin{bmatrix} w_1(x) & \dots & 0 \\ \dots & \dots & \dots \\ 0 & \dots & w_N(x) \end{bmatrix}_{N \times N} \text{ diagonal matrix} \quad (25)$$

and

$$Y = \{y_1, y_2, \dots, y_N\} \quad (26)$$

Minimizing the norm $J(x)$ in Equation (10) with respect to $a_m(x)$ leads to the following linear relation between $a_m(x)$ and y

$$A(x) a_m(x) = B(x) Y \quad (27)$$

where the matrices $A(x)$ and $B(x)$ are defined by

$$A(x) = P^T W P = \sum_{i=1}^N w_i(x) p(x_i) p^T(x_i) \quad (28)$$

$$B(x) = P^T W = [w_1(x)p(x_1) \quad w_2(x)p(x_2) \quad \cdots \quad w_N(x)p(x_N)] \quad (29)$$

The unknown coefficients $a_m(x)$ can be obtained by solving Equation (27), which results in

$$a_m(x) = A^{-1}(x) B(x) Y \quad (30)$$

Substituting the unknown coefficient from Equation (30) into the Equation (21) leads the MLS interpolation of the $s(x)$ as

$$s(x) = P^T(x) A^{-1}(x) B(x) Y \quad (31)$$

The MLS approximation given in Equation (31) is well defined only when the matrix A is non-singular. This is true only if there are at least n sampling points in the influence domain of a node X_i such that $n \geq m$. For example, for a one-dimensional case with a linear basis function ($m=2$), the value of n should be ≥ 2 . For a quadratic basis function in a two-dimensional case, the value of n should be ≥ 6 .

Except for the weight function $w_i(x)$, all other quantities in the MLS approximation are well defined. As already mentioned, the weight function is non-zero only in the influence domain of a node i , and equal to zero outside the influence domain. In the present study, the influence domain is assumed to be a sphere with radius l_i . The radius l_i must be large enough to contain at least m nodes in each direction of the parametric space. The weight function is selected such that its value goes from unity at the center of the influence domain to zero at the boundary and outside the influence domain. This property of the weight function makes MLS a local approximation compared to the GLS approximation traditionally used to represent the entire domain by a single function. It may be noted that in the MLS method for every new interpolation point ($s(x)$) Equation (31) is formed and solved.

In this paper, three spline functions with C^1, C^2 , and C^3 continuity are used as weight functions

For C^1 :

$$w_i(x) = \begin{cases} 1-3r_i^2+2r_i^3 & 0 \leq r_i \leq 1 \\ 0 & r_i > 1 \end{cases} \quad (32)$$

For C^2

$$w_i(x) = \begin{cases} 1-10r_i^3+15r_i^4-6r_i^5 & 0 \leq r_i \leq 1 \\ 0 & r_i > 1 \end{cases} \quad (33)$$

For C^3

$$w_i(x) = \begin{cases} 1-35r_i^4+84r_i^5-70r_i^6+20r_i^7 & 0 \leq r_i \leq 1 \\ 0 & r_i > 1 \end{cases} \quad (34)$$

where $r_i = \frac{|x_i - x|}{l_i}$ is the normalized distance, from the center of the influence domain (x_i) and a general point x .

The smoothness of MLS approximation is controlled by both the weight and basis functions. The precision (continuity) of MLS interpolation will be equal to the minimum precision of the weight and basis function.

3. Progressive Lattice Sampling (PLS) Experimental Design:

The selection of sampling points plays a major role in the accuracy of a response surface. There are many schemes available in the literature. In this study the Progressive Lattice Sampling (PLS) incremental experimental design sequence from reference 2 will be used. The PLS scheme is shown in Figure 4 for two variables X_1 and X_2 . In this example, the square represents the parameter space of X_1 and X_2 . Level 1 of the design consists of three samples, with one sample in the center of the parameter space and two other samples along the boundary. For d parameters, Level 1

requires $d + 1$ samples. Level 2 adds d samples to complete a $2d + 1$ “simple-quadratic” layout. Level 3 adds a 2^d factorial design. Level 4 adds a Box-Behnken design to complete an over all 3^d full factorial design. (In 2-D, Levels 3 and 4 have the same layout) Level 5 adds a sub-scaled 2^d factorial design as shown in the figure. Level 6 adds the appropriate samples to complete a 5^d full factorial design. Level 7 adds a sub-scaled 4^d full-factorial design in the interior of the parameter space as shown. The strength of PLS is that it provides an efficient way to add sample sites that leverage previous samples so that uniform distribution of the samples over the parameter space is maintained.

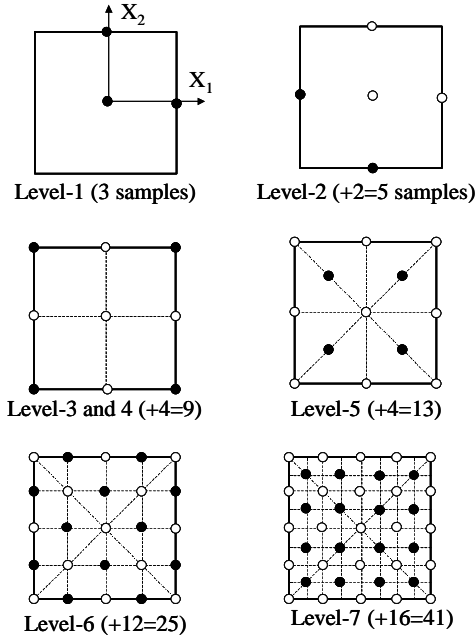


Figure 4. Progressive Lattice Sampling Points

4. Application Problems:

Two numerical examples, one with two design variables and another with four design variables are considered. Response surfaces are constructed and compared using RBF with or without augmented polynomial terms. For each problem, the response obtained using RBF is compared with response obtained using GLS, kriging and MLS methods. Interpolating at an arbitrary number of points and comparing them with reference solutions measure the accuracy of each response surface.

4.1 Two-Variable Problem:

First the described interpolation methods are applied to a two-design variables problem selected from reference 2.

The target response function for the two-variables is shown in Figure 5

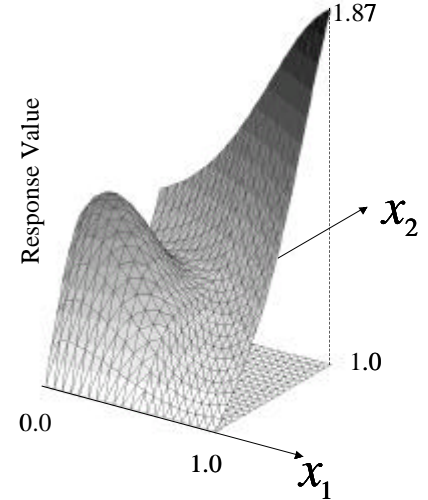


Figure 5. Target Response Function for Two-Variables Problem

This response function is defined as:

$$\begin{aligned} & \text{response}(X_1, X_2) \\ &= \left[0.8r + 0.35 \text{Sin} \left(\frac{2.4pr}{\sqrt{2}} \right) \right] [1.5 \text{Sin}(1.3q)] \end{aligned}$$

on the domain $0 \leq X_1 \leq 1, 0 \leq X_2 \leq 1$

$$\text{with } r = \sqrt{X_1^2 + X_2^2}, q = \text{arc tan} \left(\frac{X_2}{X_1} \right) \quad (35)$$

Exact data values of this function are obtained at the PLS sampling points shown in Figure 4. The response surface is generated for each of the various PLS levels in Figure 4. The response surface is then used to interpolate the value at any other point.

Table 2: Average Percent Error for Radial Basis Functions Without Polynomial Terms

Number Of Sampling Points	Radial Basis Function Type						
	Linear	Cubic	Thin Plate Spline	Gaussian	Multiquadratic	Compact-I	Compact-II
9	27.91	21.12	19.44	28.38	30.68	33.00	33.57
13	13.06	7.52	8.64	6.22	10.68	6.27	5.05
25	6.02	1.75	2.29	1.01	4.31	2.49	2.80
41	2.56	0.56	0.80	0.24	3.65	0.48	1.17

Table 3: Average Percent Error for Radial Basis Functions With Polynomial Terms

Number Of Sampling Points	Polynomial Augmented Radial Basis Function Type						
	Linear	Cubic	Thin Plate Spline	Gaussian	Multiquadratic	Compact-I	Compact-II
9	27.01	23.22	23.86	22.54	21.94	25.23	29.00
13	11.02	9.20	9.71	8.48	10.17	9.12	8.57
25	4.82	2.26	2.734	1.25	4.92	2.16	2.26
41	2.15	0.63	0.87	0.24	1.81	0.59	0.78

To examine the fitting performance (within the PLS framework) of the various response surface construction methods, a global measure of average error is defined as follows:

$$Average\ percent\ Error = \frac{\sum_{i=1}^N |(exact)_i - (predicted)_i|}{\sum_{i=1}^N |(exact)_i|} \times 100.0 \quad (36)$$

Where “exact” in the summation comes from the evaluation of the exact function. The predicted values in the summation come from the response surface approximation at N interpolated points. For this example N is set to equal to 441 and selected from equally spaced points on a 21x21 square grid overlaid on the domain. Earlier experience in reference 2 indicates the 21x21 grid appears to be sufficiently dense to achieve adequate representation of the target and approximate functions.

Four levels with 9, 13, 25 and 41 sampling points were selected for comparison. Response surfaces were constructed using augmented RBF, classical RBF, GLS, kriging and MLS methods for all the four levels sampling points selected. The average errors were calculated by interpolating the response surfaces at 441 points using Equation (24).

First response surface were generated for RBF without polynomial terms. The average errors obtained for the classical and compactly supported RBF are shown in Table 2. All the RBF methods that did not include polynomial terms produced almost the same percentage of error for a given number of sampling points. Hence, a mean curve passing through the average errors is plotted in Figure 6.

From Figure 6, the mean curve represents the best fit for all the RBF types except for sampling points less than 15. This implies virtually all the RBF without polynomial terms produce identical response prediction. Both the classical and compactly supported RBF functions produced almost identical responses.

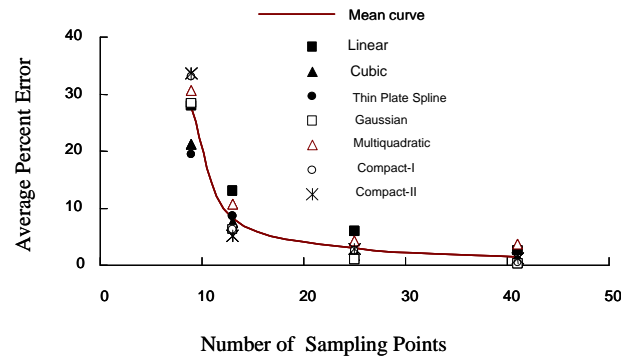


Figure 6. Average curve representing the mean values of the errors

Next, response surfaces were constructed using polynomial augmented RBF. The radial basis functions are augmented with cubic polynomial for the 13, 25 and 41 sampling points and quadratic polynomial for 9 sampling points. The average errors obtained for the various RBF for the selected sampling points are given in Table 3. Here also, all the augmented RBF types produced almost the same percentage of error for a given number of sampling points

The response produced by augmented RBF and RBF without polynomial terms are compared in Figure 7, using the mean curves passing through the errors.

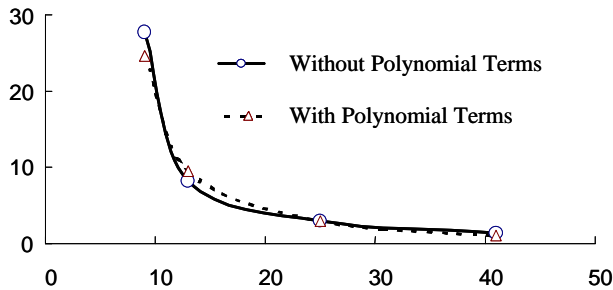


Figure 7. Variation of average mean error for augmented RBF and classical RBF

From Figure 7, the augmented RBF and RBF without polynomial terms produce nearly same error for a given number of sampling points. For both the cases, the average error decreases as the number of sampling points increased. Even though, there is no clear advantage in using augmented RBF for this problem, introduction of polynomial terms may help to reproduce the polynomial functions accurately. Note that, the augmented polynomials do not require additional sampling points for the surface construction.

Next the average errors from the augmented RBF are compared with the other response surface methods (GLS, kriging, and MLS) in Figure 8. The global GLS method consistently performs very poorly for all the sampling. The local RBF, kriging and MLS methods produced almost identical errors for a given number sampling point.

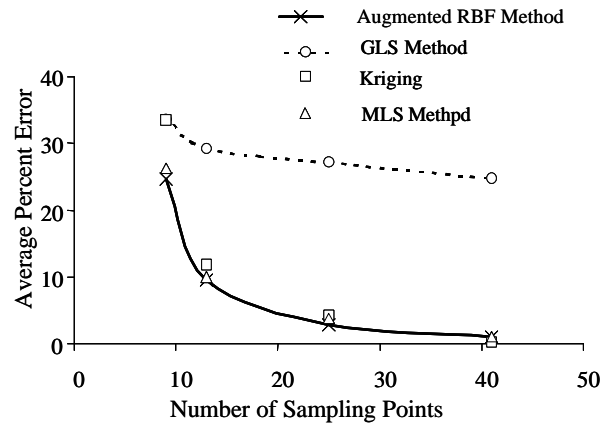


Figure 8. Comparison of RBF methods with GLS, Kriging and MLS methods for two variable problems

4.2 Four-Variables Problem:

The next example considered is a four-variable problem that is taken from the reliability-based design of a metallic, plate-like wing to meet strength and flutter requirements [14]. In this paper, only strength requirement will be considered. The selected plate-like wing configuration is shown in Figure 9.

The dimensions used for wingspan (L), wing root chord (C_R), tip chord (C_t), and sweep of the leading edge (Φ) are also show in Figure 9. The modulus of elasticity is $10 \times 10^6 \text{ psi}$ and Poisson's ratio is 0.30. The wing is clamped at the root and subjected to a uniform pressure of 1 psi .

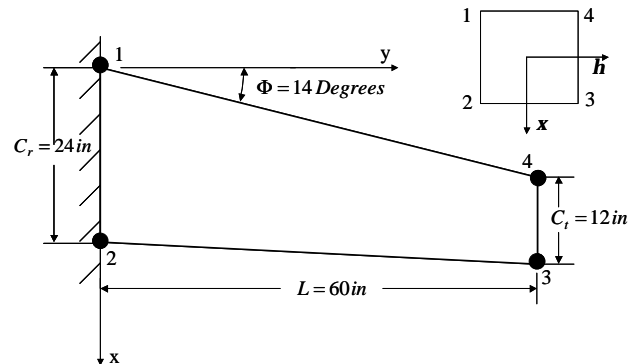


Figure 9. Dimension of Metal Plate-Like Wing

The thickness distribution along the span of the wing is assumed as bi-linear and can be defined in terms of the thicknesses of the corner nodes 1 to 4 (see Figure 9) as

$$t(\mathbf{x}, \mathbf{h}) = c_1 + c_2 \mathbf{x} + c_3 \mathbf{h} + c_4 \mathbf{x} \mathbf{h} \quad (37)$$

where

$$c_1 = \frac{(t_1 + t_2 + t_3 + t_4)}{4} \quad (38)$$

$$c_2 = \frac{(-t_1 + t_2 + t_3 - t_4)}{4}$$

$$c_3 = \frac{(-t_1 - t_2 + t_3 + t_4)}{4} \quad (39)$$

$$c_4 = \frac{(t_1 - t_2 + t_3 - t_4)}{4} \quad (40)$$

The equation relating the (x, y) and (\mathbf{x}, \mathbf{h}) wing coordinates (see Figure 9) can be written as

$$\mathbf{x} = \frac{2L(x - y \tan f)}{C_r L - (C_r - C_t)y} - 1 \quad (41)$$

$$\mathbf{h} = \frac{2y}{L} - 1 \quad (42)$$

where $-1 \leq \mathbf{x} \leq 1$, and $-1 \leq \mathbf{h} \leq 1$

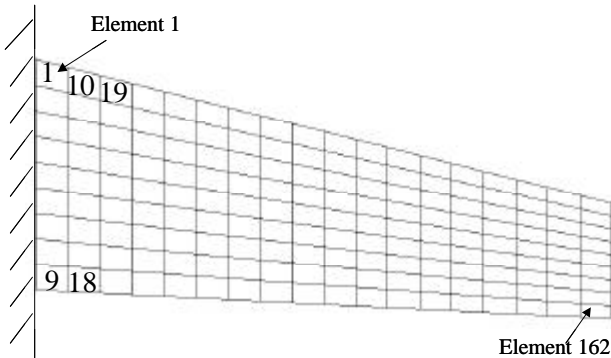


Figure 10. Finite Element Model for Stress Prediction

The four corner node thicknesses $(t_1$ to t_4) are the design variables. Each thickness is allowed to vary between

0.15 in and 0.4 in. The sampling points are generated using the PLS scheme for level-5 with 97 sampling points and level-7 with 881 sampling points. In order to predict the stress distribution as function of four design variables $(t_1$ to t_4), the plate is divided into 162 quadrilateral finite elements as shown in Figure 10. Finite element analyses with 162 quadrilateral elements are used to obtain the stresses at the centroids of each element. For example, for the 881 sampling points in level-7, 881 finite element analyses are performed. These 881 centroidal stresses for an element are used to construct the responses for that element. Hence, a total of 162 response surfaces are constructed, one for each element. The MSC/NASTRAN structural analysis code with 8-node quadrilateral elements is used for the finite element analyses.

The 162 response surfaces are generated using the five classical radial functions given in Table 1 and two Compact-I (Equation (7)) and Compact-II (Equation (8)) radial functions. In order to determine the error in the response surface estimation, 2500 random points are selected. Exact stresses are calculated using MSC/NASTRAN and predicted stress are calculated by interpolating the response surfaces. The average and %error for each element are calculated by using the following equations.

$$\text{Average Error} = \frac{\sum_{i=1}^N |(exact)_i - (predicted)_i|}{N} \quad (43)$$

$$\text{Mean Stress for an element} = \frac{\sum_{i=1}^{2500} |exact\ stress|}{2500} \quad (44)$$

The percent error is calculated as

$$\text{Average \% Error for an element} = \frac{\text{Average Error}}{\text{Mean Stress}} \times 100 \quad (45)$$

The average error for element 1 (see Figure 10) is compared in Figure 11 for 97 sampling points for RBF with and without augmented polynomial terms. Using Figure 11, the polynomial augmented RBF produced less error in the response prediction than the RBF without

polynomial terms. The variation between different types is smaller for the augmented RBF than the RBF without polynomial terms.

A similar trend is noticed in Figure 12 for the 881 sampling points. It can be seen from Figure 12 that all the RBF estimated the response within two percent. The effect of polynomial terms is more pronounced in the compact support RBF, where the error is reduced more than four times from RBF without polynomial terms.

Finally the average errors from the augmented RBF are compared with kriging and MLS methods in Figure 13. The augmented RBF functions out perform the kriging method and almost produce the same response as that of MLS method.

5. Discussion

The first example studied here not clearly established the need for augmented polynomial terms in the RBF. However, the second example clearly demonstrated that the polynomial augmented RBF function performs better than the RBF without polynomial terms. All the RBF function types produced identical performance. However, careful examination of results suggests the cubic classical function is computationally efficient and is very accurate. The importance of the positive definite property of the compact support RBF is not studied using the two examples in this paper. Further study is warranted on the importance of the positive definiteness of the RBF. In order to assess the effectiveness among RBF, MLS and kriging methods, more study should be conducted to measure the derivative generation capability of these methods to estimate sensitivity in reliability and optimization problems

6. Conclusion:

A radial basis response surface construction method using augmented and compact support Radial Basis Functions (RBF) was developed. The RBF based response surface construction was tested in two numerical examples and found to produce accurate response estimation. The polynomial augmented radial functions generally produce less error in response prediction than the classical radial and compact radial functions. The RBF response surface method was compared to local Moving Least Square (MLS), kriging, and Global Least Square (GLS) methods. The GLS method performed poorly. The local RBF, kriging and MLS methods predicted the response very accurately. All three local methods produced nearly the same error.

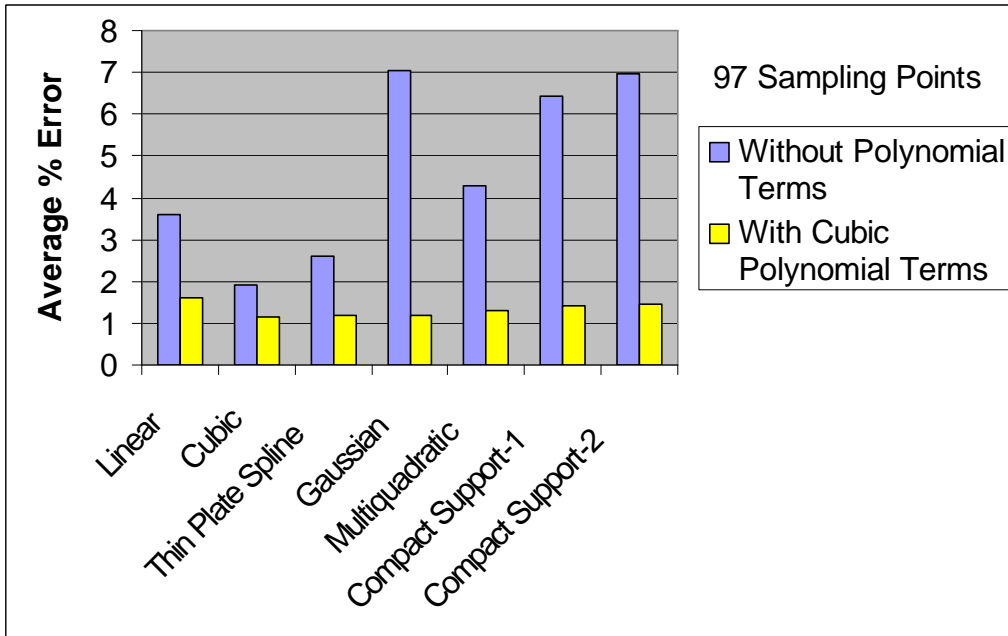


Figure 11. Average error comparison for RBF with and without augmented polynomial terms: 97 sampling points

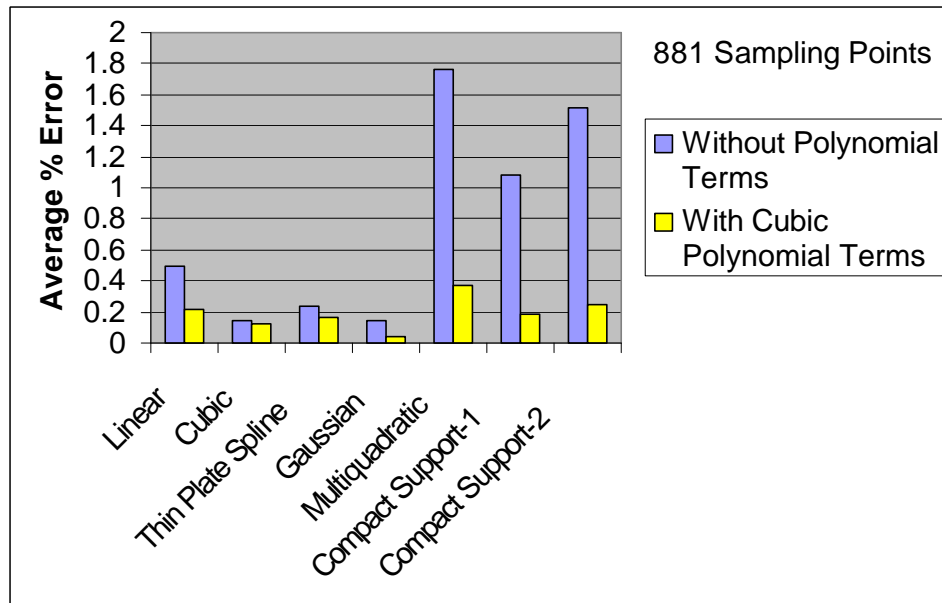


Figure 12. Average error comparison for RBF with and without augmented polynomial terms: 881 sampling points

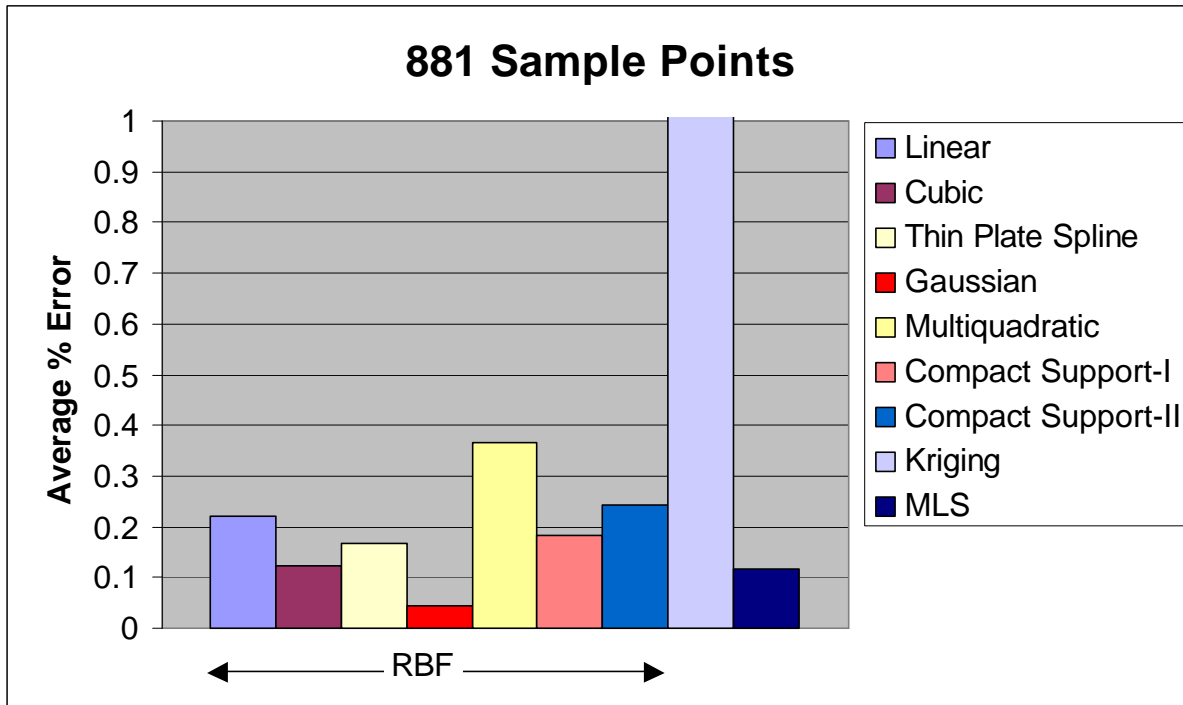


Figure 13: Average error comparison for classical and polynomial augmented radial functions

7. References

1. Stroud, W. Jefferson, Krishnamurthy, T., and Smith, Steven A., "Probabilistic and Possibilistic Analyses of the Strength of a Bonded Joint", AIAA-2001-1238, Presented at 42nd AIAA/ASME/ASCE/AHS/ASC Structures, Structural Dynamics, and Materials Conference, April 16-19, 2001, Seattle, WA. Available on CDROM Vol. 6, No. 2, AIAA, Reston, VA
2. Krishnamurthy, T., Romero, V. J, " Construction of Response Surface with Higher Order Continuity and its Application to Reliability Engineering", AIAA-2002-1466, Presented at 43rd AIAA/ASME/ASCE/AHS/ASC Structures, Structural Dynamics, and Materials Conference,, April 22-25, Denver, CO, 2002.
3. Giunta, Anthony A., and Watson, Layne T., "A Comparison of Approximation Modeling Techniques: Polynomial versus Interpolating Models", paper AIAA-98-4758, presented at the 7th AIAA/USAF/NASA/ISSMO Symposium on Multidisciplinary Analysis and Optimization, St. Louis, MO, Sept. 2-4, 1998.
4. McDonald, D. B. , Grantham, W. J. , Tabor, W. L. , and Murphy, M. J. , " Response Surface Model Development for Global/Local Optimization Using Radial Basis Functions", AIAA-2000-4776, 8th AIAA/USAF/NASA/ISSMO Symposium on Multidisciplinary Analysis and Optimization, Sep. 6-4, Long Beach, CA, 2000.
5. Hussain, M F. , Barton, R. R, Joshi, S. B., " Metamodeling: Radial Basis Functions, Versus Polynomials", *European Journal of Operational Research*, pp. 142-154, 2002.
6. Wang, Ping Po, "Parameter Optimization in Radial Basis Function Response Surface Approximation", AIAA-2002-1344, Presented at 43rd AIAA/ASME/ASCE/AHS/ASC Structures, Structural Dynamics, and Materials Conference, April 22-25, Denver, CO, 2002.
7. Powell, M, J. D., "The Theory of Radial Basis Function Approximation in 1990", *Advances in Numerical Analysis*", Vol. II, "Wavelets, Subdivision Algorithms, and Radial Basis Function", Edited by Will Light, Clarendon Press, Oxford, 1992, Chapter 3, pp. 105-210.

8. Wu, Z., "Compactly Supported Positive Definite Radial Function", *Advances in Computational Mathematics*, pp. 283-292, 1995.
9. Wendland, H., "Piecewise Polynomial, Positive Definite and Compactly Supported Radial Functions of Minimal Degree", *Advances in Computational Mathematics*, pp. 389-396, 1995.
10. Wendland, H., "On the Smoothness of Positive Definite and Radial Functions", *Journal of Computational and Applied Mathematics*, pp. 177-188, 1999.
11. Atluri, S N., and Zhu, T., "A new meshless Local Petrov-Galerkin (MLPG) approach in Computational Mechanics", *Computational Mechanics*, Vol. 22, pp. 117-127, 1998.
12. Raju, I. S. , and Chen, T., " Meshless Petrov-Galerkin Method Applied To Axisymmetric Problems", 42nd AIAA/ASME/ASCE/AHS/ASC Structures, Structural Dynamics, and Materials Conference, AIAA Paper No. 2001-1253, April 16-19, Seattle, WA, 2001
13. Choi, K. K. Youn, B., and Yang, R-J. "Moving Least Squares Method for Reliability-Based Design Optimization", *Fourth World Congress of Structural and Multidisciplinary Optimization, Dalian, China, June 4-8, 2001.*
14. Stroud, W. Jefferson, Krishnamurthy, T., Mason, B. H, Smith, S. A., and Naser, S. Ahamad, "Probabilistic Design of a Plate-Like Wing to Meet Flutter and Strength Requirements", AIAA-2002-1464, Presented at 43rd AIAA/ASME/ASCE/AHS/ASC Structures, Structural Dynamics, and Materials Conference, April 22-25, Denver, CO, 2002.